Hindawi
Advances in Materials Science and Engineering
Volume 2022, Article ID 8591973, 13 pages
https://doi.org/10.1155/2022/8591973

Research Article

Analysis of Stress-Strain Relationship of Earthen Soil Based on Molecular Dynamics

Jianwei Yue,[1,2] Xuanjia Huang,[1] Peng Li ,[1,2] and Tingting Yue[2]

[1]*School of Civil Engineering and Architecture, Henan University, Kaifeng, Henan 475004, China*
[2]*Key Laboratory for Restoration and Safety Evaluation of Immovable Cultural Relics in Kaifeng, Henan University, Kaifeng, Henan 475004, China*

Correspondence should be addressed to Peng Li; chipren@163.com

Received 23 July 2021; Accepted 24 February 2022; Published 25 March 2022

Academic Editor: Qian Chen

The calibration of material mechanical parameters and deformation and failure mechanism of earthen soil have always been difficult problems in the field of cultural relics protection. How to establish a relationship between physical and mechanical properties of soil at macro and micro scales is the focus of the research. The nanostructure model of earthen soil composed of many atoms was established by molecular dynamics (MD) method. The stress-strain relationship of different moisture content was obtained by uniaxial compression simulation. Based on the electron micrograph image (magnification ×500) and the image reconstruction method, a micromodel composed of particles and pores was constructed. Furthermore, using the displacement loading method, we obtained the stress-strain relationship of the earthen soil with different moisture contents. Our results showed that the displacement of the left and right boundaries of the circular pore model is 1.26 times more than that of the polygonal pore model, and the displacement of the polygonal pore model is 1.28 times more than that of the circular pore model. The stress-strain curve simulated by the polygonal pore model is consistent with the experimental results. The results of the numerical analysis are in good agreement with those of the macro test, which indicates that the research ideas and the methods used for earthen soil exploration in this work are feasible. Our present findings provide reference for deterioration research and safety evaluation of cultural relic buildings such as earthen sites.

1. Introduction

Soil sites are significantly affected by the environment, and soil sites are unique and nonrepeatable [1]. A large number of samples cannot be taken on the existing soil sites, which makes the research progress of soil mechanical properties of undisturbed sites slow. MD is a new micromechanical method developed in recent years. Its purpose is to obtain the required macroscopic physical and mechanical quantities of the object through long-time operation of a few particles [2]. With the help of theoretical calculation method and molecular dynamics simulation, the research information from multiple angles (microstructure, dynamics, etc.) and multiple levels (from microatomic level to macrostatistical level) is obtained [3] (Figure 1), so as to save the test cost and increase the test efficiency.

Theoretical and experimental research has been performed on the macromechanical properties of earthen soil. For example, Song et al. [4] conducted a macroscopic assessment on the soil mechanical characteristics of sites in Northwest Henan Province, China. In addition, Yue et al. [5] established a theoretical model of slope failure cusp catastrophe based on elastic sliding mass. However, fewer studies have been done on the microscale physical and mechanical properties, and the deterioration mechanism of earthen soil has not been elucidated. With the rapid development of computer technology, numerical simulation of complex mechanical behavior can effectively eliminate the influence of human and environmental factors in physical tests, better simulate the damage and failure process of microstructures, and fulfill the purpose of studying the characteristics of earthen soil foundation. The establishment of the

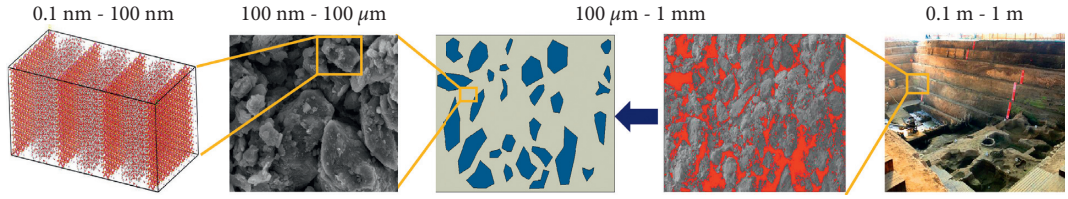

Figure 1: Multiscale structural characteristics of site soil materials.

constitutive relationship and numerical model of the materials of the earthen soil is not only the first step to meeting engineering application requirements but an important factor affecting numerical simulation results.

Many scholars have carried out a lot of research work around the physical and mechanical properties and structural characteristics of soil [6, 7]. The research trend shows the characteristics of multiscale integration, multimethod combination, and multidisciplinary intersection. The research shows that the microbehavior plays an extremely important role in the mechanical properties of soil. The research method of "combination of macro and micro" has become the mainstream of soil mechanical properties research at present and even in the future [8, 9]. Shen et al. first introduced the damage theory for research of soil sample constitutive models and established the elastic-plastic damage model [10] and nonlinear damage mechanics model [11]. Furthermore, Kuang et al. [12] carried out molecular dynamics (MD) simulation on the water molecular structure between crystal layers of montmorillonite minerals with different water content, and revealed the basic mechanism of high-pressure mechanical properties of clay from multiscale level. Yang et al. [13] used molecular dynamics simulation to study the hydration properties and adsorption properties of clay minerals, and clarified the structure and dynamic properties of clay in hydration. Liu et al. [14] applied molecular dynamics to study the influence relationship between the connection characteristics of soil particles (structural units) and the deformation and failure characteristics of soil, and found that the macromechanical properties of soil are controlled by the microstructure of soil. The structural fracture surface of soil passes through the connection surface between particles and particle aggregates, not through the particles themselves, that is, the weakest part of the connection between particles is destroyed first. In addition, Tang et al. [15] evaluated the microstructure and mechanical changes of expansive soil under multiscale cyclic loading and established a unified expression of stress-strain characteristics reflecting soil macrostructure and microstructure and considering microdamage. Chen [16] analyzed the elastoplastic constitutive model of soil samples based on numerical and physical simulation; the author also elaborated the relationship between physical and numerical simulation of soil samples. Zhao et al. [17] used molecular dynamics method to establish a variety of molecular models in Materials Studio software to analyze the influence of interlayer cation types on water molecules adsorbed by montmorillonite.

The aforementioned research results have promoted the development of research on mechanical properties of macrosoil and microsoil samples to a certain extent. However, in view of the complexity and variability of soil samples [18], the intraparticle earthen soil cement has been simplified to a certain extent in the established models; the influence of the environment on cement has also been neglected. Obviously, deeper knowledge is needed on the microscale stress variation law of the soil sample and its components [19]. In previous studies, we found that the stress and strain results of earthen soil samples were different when diverse water samples were used. As can be seen in Figure 2, the compressive strength of the soil samples made with pure water is higher than that of the soil samples prepared with pit water from the site. The decrease in their moisture content made these differences even more obvious.

First, earthen sites are unique. On-site sampling would disturb the site body and is hence limited by the requirements of cultural relic protection. Thus, the number of soil samples taken from such site cannot be large, resulting in low test repeatability and slow progress of research on the mechanical properties of undisturbed earthen soil. Second, cements exist widely in natural geotechnical materials, and intergranular cementitious materials have an important impact on the mechanical properties of geotechnical materials. However, the cost of micromechanical model tests is high, hindering appropriate observations of the microevolution law of cementation failure. Therefore, based on the idea of Molecular dynamics (MD) simulation method, in this paper, with the help of material studio 7.0 simulation software, we established the nanostructure model of Zhouqiao earthen soil and applied lamps software to analyze the mechanical properties of Zhouqiao earthen soil; based on the SEM image of earthen soil and a small number of mechanical test results, a micromodel composed of particles, cements, and pores was established. Furthermore, we assessed the method for the determination of the microscale mechanical properties of the intraparticle earthen soil cement.

2. Construction and Simulation of Molecular Dynamics Model

2.1. Modeling Basis. By comparing the electron microscope images of soil samples under different magnification, the differences of microstructure of soil samples under different orders of magnitude are studied. For heterogeneous geotechnical materials, when the material is transformed into an image, different substances in the material can be reflected in the image through the change of gray or color, and the image reproduces the structural characteristics of the material well. Using digital image technology, the gray image of SEM is

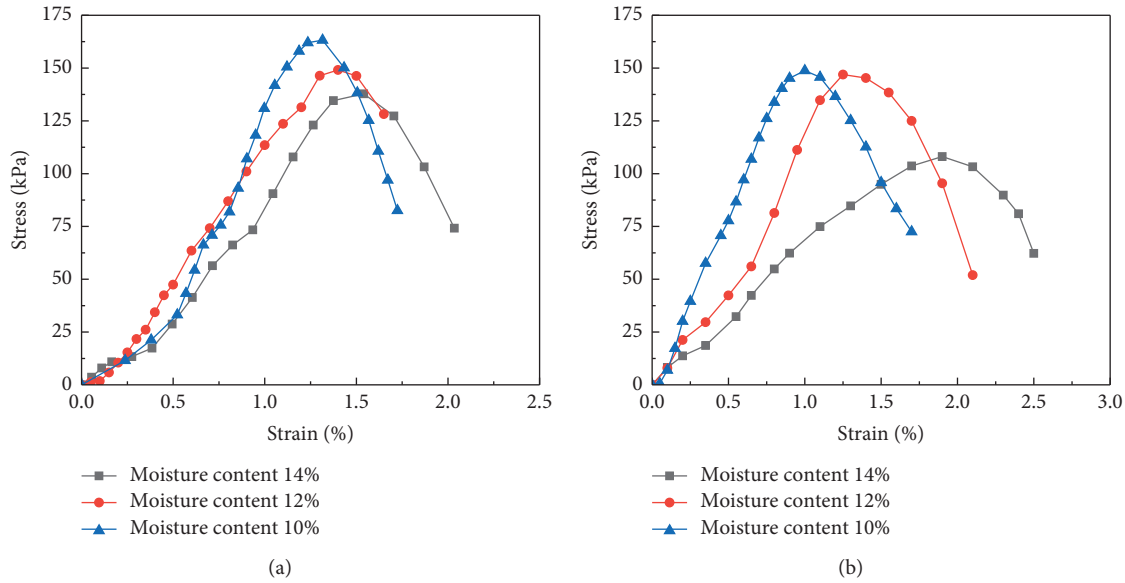

Figure 2: Stress-strain results of site soil samples: (a) sample made with pure water and (b) samples prepared with pit water from the site.

regarded as a three-dimensional coordinate system in MATLAB software. The length and width of the image are X and Y coordinate axes respectively, the gray value of the image is regarded as Z axis, and the gray value is regarded as $Z = f(x, y)$. After three-dimensional simplification of the gray image, the integral value of a three-dimensional irregular body with two-dimensional image size as the bottom and threshold as the high is calculated. The microstructure distribution image of soil sample in Figure 3 is transformed into a three-dimensional real microstructure diagram (Figure 4). Figure 4 shows the three-dimensional structural characteristics of soil samples. It can be obtained from Figures 4(a) to 4(e). With the increase of the magnification of the SEM image, the yellow and green parts gradually decrease, and the threshold tends to a certain range, which is reflected in the gradual simplification of the soil sample information contained in the picture, and the soil sample can only be determined as heterogeneous material in the macro state. When a certain observation scale is reached, the soil sample can be assumed to be soil sample and pore. The nano model of soil sample is constructed using Materials Studio software, and the mechanical properties of soil sample under different moisture content are studied by Monte Carlo method and molecular dynamics method. The research results provide data support for the subsequent microscale model.

Zhang et al. [20] studied the pore type, scale, and shape of clay and proposed that the pores contained in clay mineral structure can be divided into three types: intergranular pores formed by mineral particle compaction and deposition. Clay intergranular pores formed during diagenetic transformation of minerals. The gap (layer spacing) caused by the distance between crystal layers in clay crystal and the relationship between various pores is shown in Figure 5. Li et al. [21] found that most montmorillonite clay minerals are in flake structure and stacked into montmorillonite basic particles. The thickness of the wafer layer is 1 nm, and the length and width are tens to hundreds of nanometers. When the crystal layer contains water, it can expand to produce interlayer nanopores with different thicknesses of about 0.2 to 2 nm. The research results of the aforementioned scholars provide a basis for the establishment of molecular models at the nanoscale.

2.2. Modeling. Based on the research of Bish et al. [22], the main component of silty clay is clay based mineral montmorillonite, and the geometric configuration of crystal is shown in Figure 6. In this work, the initial model of soil sample is based on montmorillonite, and the random water molecule modeling of Monte Carlo method is carried out using Material Studio software and setting the water molecule density as 1 g/cm^3 in the amorphous cell module at room temperature 298 K. The montmorillonite molecular model and random water molecule model are superimposed using the build layers function. Based on the density of soil samples with different moisture content, the molecular models of 10%, 12%, 14%, and 16% moisture content are established respectively. The atomic number and density of the model are shown in Table 1. Finally, discover setup is used to establish the force field and discover minimization is used to minimize its energy. In order to avoid the influence of periodic boundary in the process of uniaxial compression, the initial model of soil sample with water content is amplified by supercell, so that the size of molecular model reaches the visualized soil sample in microscale [23]. The simulation area size of the final initial model of soil sample is $A = 104$ Å, $B = 89$ Å, $C = 118$ Å, $\alpha = 90^\circ$, $\beta = 90^\circ$, and $\gamma = 90^\circ$, as shown in Figure 7. In Figure 6, the yellow ball, red ball, purple ball, and white ball represent silicon atom, oxygen atom, aluminum atom, and hydrogen atom, respectively. In Figure 7, the purple part is the crystal layer and the yellow

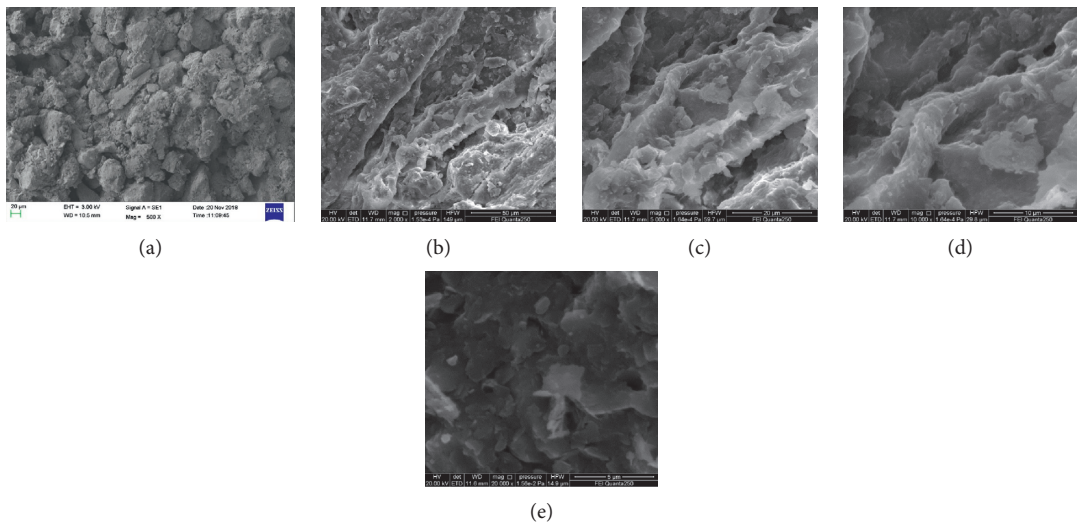

(a) (b) (c) (d)

(e)

Figure 3: Distribution of the soil particle structure at the macroscale and microscale at different magnifications: (a) 500 times magnification, (b) 1000 times magnification, (c) 3000 times magnification, (d) 5000 times magnification, (e) and 10,000 times magnification.

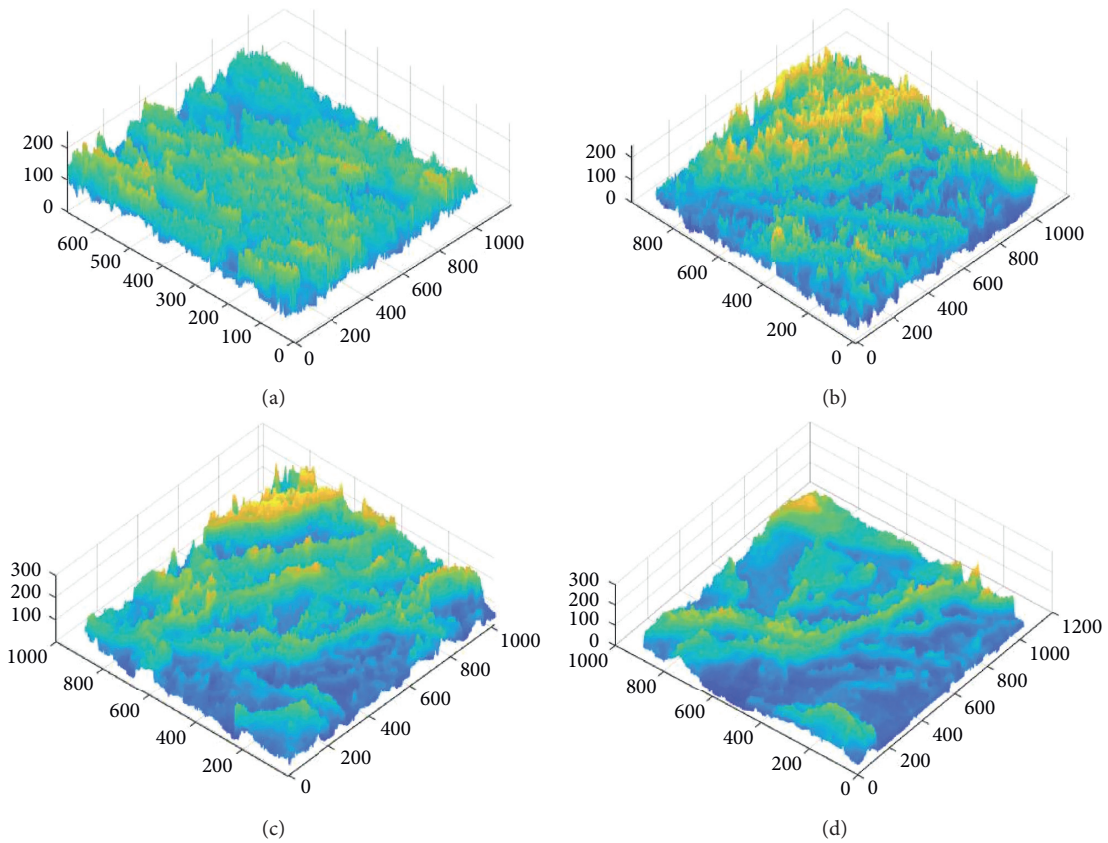

Figure 4: Continued.

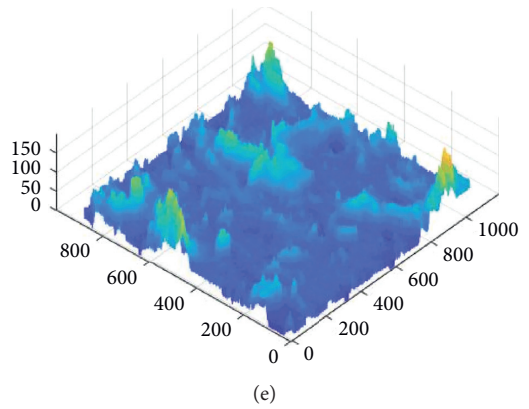

Figure 4: Three-dimensional structural characteristics of soil sample: (a) 500 times magnification, (b) 1000 times magnification, (c) 3000 times magnification, (d) 5000 times magnification, (e) and 10,000 times magnification.

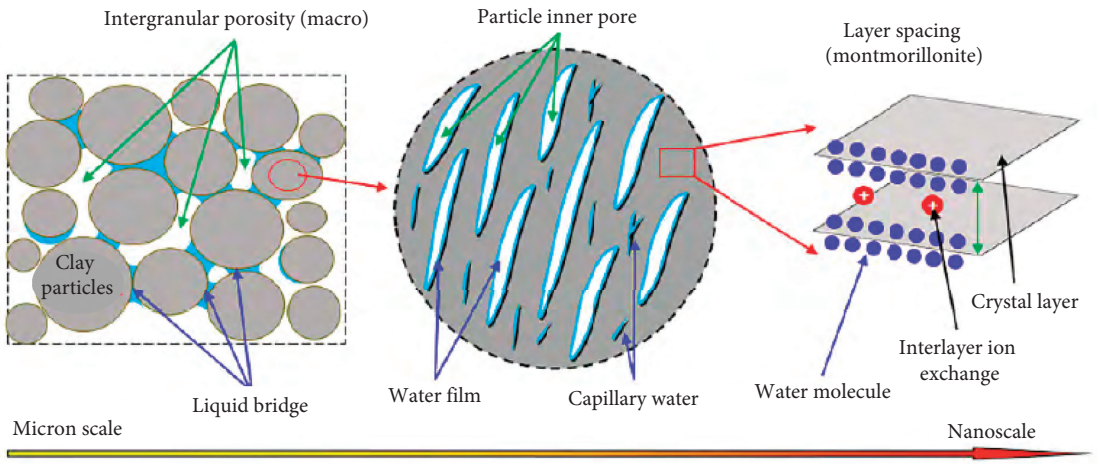

Figure 5: Characteristics of gas water distribution of clay minerals [21].

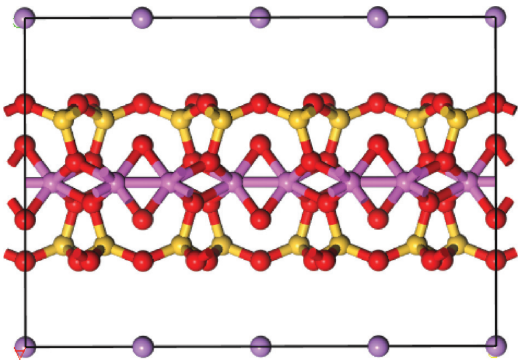

Figure 6: Unit cell of montmorillonite.

Table 1: Atomic number and density of molecular model.

Model name	Quantity of Si	Quantity of O	Quantity of Al	Quantity of Li	Quantity of H_2O	Density (g/cm^3)
10% moisture content model	6400	20,800	4800	2800	16,000	1.47
12% moisture content model					17,500	1.50
14% moisture content model					19,000	1.53
16% moisture content model					20,500	1.58

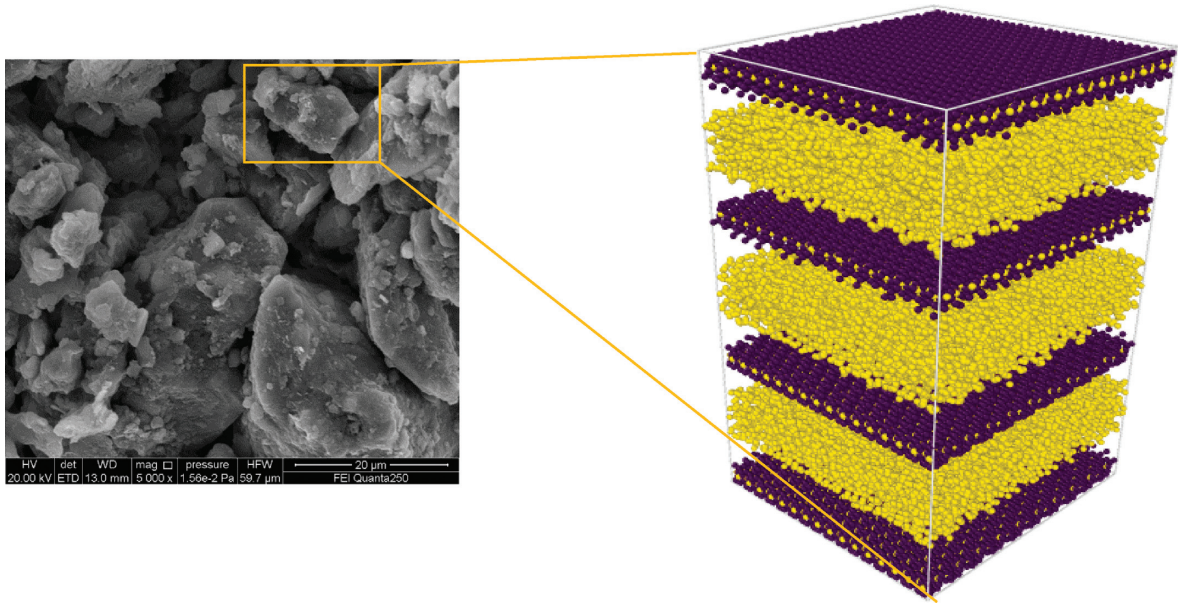

Figure 7: Initial model construction intention of soil sample.

part is the water layer. Through uniaxial compression simulation of the model, the stress-strain relationship of the molecular model is obtained, as shown in Figure 8.

3. Construction of the Microscale Simulation Model

The uniaxial compression test can simulate the most unfavorable situation of material failure under the three-dimensional unconstrained condition of the structure, and the deterioration of earthen sites is mostly concentrated on the outer surface of the soil and the quasi-brittle material (concrete damage plasticity) [24, 25]. A HITACHI S-2700 scanning electron microscope was used in this experiment, which is composed of a vacuum electron beam emission, and image generation systems (Figure 9). In this paper, the analysis is based on the numerical model building method already proposed by our group, and the specific model building process is as follows [1].

3.1. Modeling Basis. Similarly to the analysis of the physical and mechanical properties of ordinary buildings, we also need to consider the microperspective in the exploration of the relationship between microstructure and macromechanical properties. Figure 3 shows the images of soil particles under the electron microscope, within the field of view magnified by 500 times. It is clear to see the details of the particles, including the irregular cracks on the surface and the shape and size of the particles. At this scale, the particles with a diameter within 5 and 25 μm can be observed, and the corresponding pore distribution and disorderly arrangement of viscous particles is visible by the accumulated materials between particles. At further increased magnification from 1000 to 3000 times, the shape of the particles is clear, but the number of particles is low; at a magnification from 5000 to 10,000 times, the size and shape of the particles in the microstructure begin to distort, and lose their microscale guiding significance. Therefore, the microscopic modeling of earthen soil is to be based on the electron micrograph images of earthen soil at x500 magnification.

To avoid the influence of the randomness of the SEM images on the research results, when the SEM images were taken, on the basis of meeting the screening test level, the area of 1 mm × 1 mm was shot from the left to the right and from the bottom to the top. According to the pixel size area of the photo taken by ×500 magnification lens, the number of electron microscope pictures to be taken is obtained by

$$\frac{1 \times 1}{0.644 \times 0.431} \approx 4 \text{ photos.} \quad (1)$$

The determination and selection of a threshold is essential to image binarization. Owing to the different properties of objects and the diversity of gray changes in various images, it is difficult for traditional binarization methods to achieve ideal processing results. To make the processed image consistent with the structure of the real soil sample, the Image-Pro Plus 6.0 software (IPP, Media Cybernetics, Inc., Silver Spring, MD, USA) was used to process the SEM photos at 500× magnification [14]. To reduce the error caused by the randomness of the calculation results under a single threshold, the area ratio of the black and white colors was determined by adjusting the level of the cutting plane represented by the threshold value, based on the porosity. The best threshold [26] that can truly reflect the microstructure of soil was found.

3.2. Modeling. ABAQUS software was used to construct a rigid plate with a length of 0.644 mm and a two-dimensional geometric model of 0.644 mm × 0.431 mm. With the pressure equipment in the rigid plate simulation test, and the

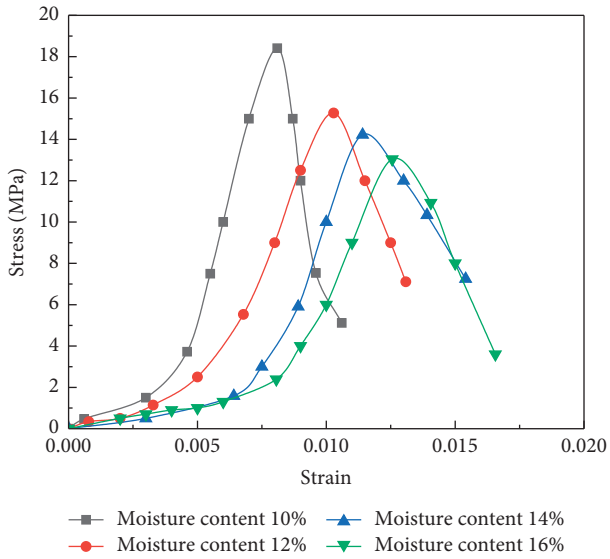

Figure 8: Stress-strain curves of molecular dynamics model.

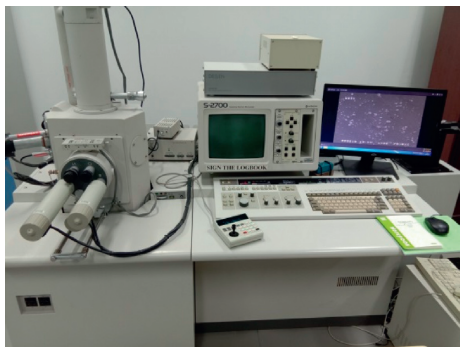

Figure 9: HITACHI S-2700 scanning electron microscope.

two-dimensional solid element was selected to provide the section attribute. The plane thickness of the rigid plate was set at 0.020 mm to simulate the uniaxial compression test.

The numerical model was composed of soil particles, pores, and cements. The soil particles were regarded as elastic rigid bodies [27]. The properties of the intraparticle cementation materials were determined by the constitutive model of concrete damage plasticity (CDP). The material parameters of each phase in the numerical simulation model were calibrated according to the specific working conditions (Table 2).

In Table 2, Ψ is the expansion angle; ϵ is the flow potential offset; f_{b0}/f_{c0} is the ratio of biaxial ultimate compressive strength to uniaxial ultimate compressive strength; K is the ratio of the second stress invariant on the tensile meridian plane to that on the compressive meridian plane; and μ is the viscosity coefficient.

In this study, vertical displacements of 0.006, 0.009, and 0.012 mm were applied to the top of the upper platen by the displacement loading method [28]. The friction coefficient was selected to be $\mu = 0.492$ [24]. After the finite-element model was established, the X direction, Y direction, and the rotation angle of the lower boundary of the model were set as fixed-end constraints. CPE4R was used as the model cell type. The initial value of increment step size was set to 0.001, and the minimum value was 1E−012. Figure 10 is the electron microscope image of Zhouqiao earthen soil, Figure 11 is the uniaxial compression test model results of soil samples with polygonal pores, and Figure 12 is the uniaxial compression simulation model results of soil samples with circular pores.

4. Simulation Verification and Analysis of the Results of the Uniaxial Compression Test

Figure 13 shows the macro test and simulation results. By comparing the results of the theoretical model and the uniaxial compression numerical model, it is found that the curve obtained by the simulation calculation of the polygonal pore model is slightly higher than the test stress-strain curve. The main reason is that the simulated strength is higher than that of the test because there are microcracks in the real soil sample, and there are no initial cracks in the model. The calculation result is reasonable.

By adding a difference interval of 10 kPa to the indoor test stress-strain curve, it can be found from Figure 13 that the curve simulated by the circular pore model deviates greatly from the indoor test stress-strain curve. The circular pore model has smooth boundary and less constraints between soil samples. With the increase of compressive load, the displacement change is more continuous, which is one of the reasons for the larger peak strain and smaller peak stress. Although there is a deviation between the results of circular pore model and indoor test results, the change law in the early stage of curve development is basically consistent because the elastic modulus of soil sample is consistent. And with the increase of soil moisture content, the coincidence degree of the result curve is also further increasing. When the moisture content is 10%, the peak strain difference is about 0.5%, and the peak stress difference is about 40 kpa; When the moisture content is 16%, the peak strain difference is about 0.2%, and the peak stress difference is about 15 kPa.

Owing to the limited space and the similarity of the work, in this paper, we have analyzed only the results of polygonal pore model 1 and circular pore model 5. Figure 14 represents the simulation results of model 1. Figure 15 represents the simulation results of model 5, the legend "+" in the axial stress diagram is the tensile stress, "−" is the compressive stress, the legend "+" in the displacement diagram is the positive direction of the coordinate axis and "−" is the negative direction of the coordinate axis. As can be seen from Figures 14(a) and 15(a), regular changes occurred in the soil displacement; the overall displacement was altered in a descending order. The bottom displacement was the smallest, whereas the upper displacement was larger. As the bottom boundary of the model was a fixed support constraint, the axial load displacement at the bottom had to be zero. In the process of uniaxial compression, the internal displacement distribution of the test block was not balanced, and the nonuniformity of the displacement increased with the increase of the load. Under the continuous action of the compression displacement, the local displacement would

Table 2: Unified hardening model parameters.

Ψ (°)	ϵ	f_{b0}/f_{c0}	K	μ
30	0.1	1.16	0.6667	0.0005

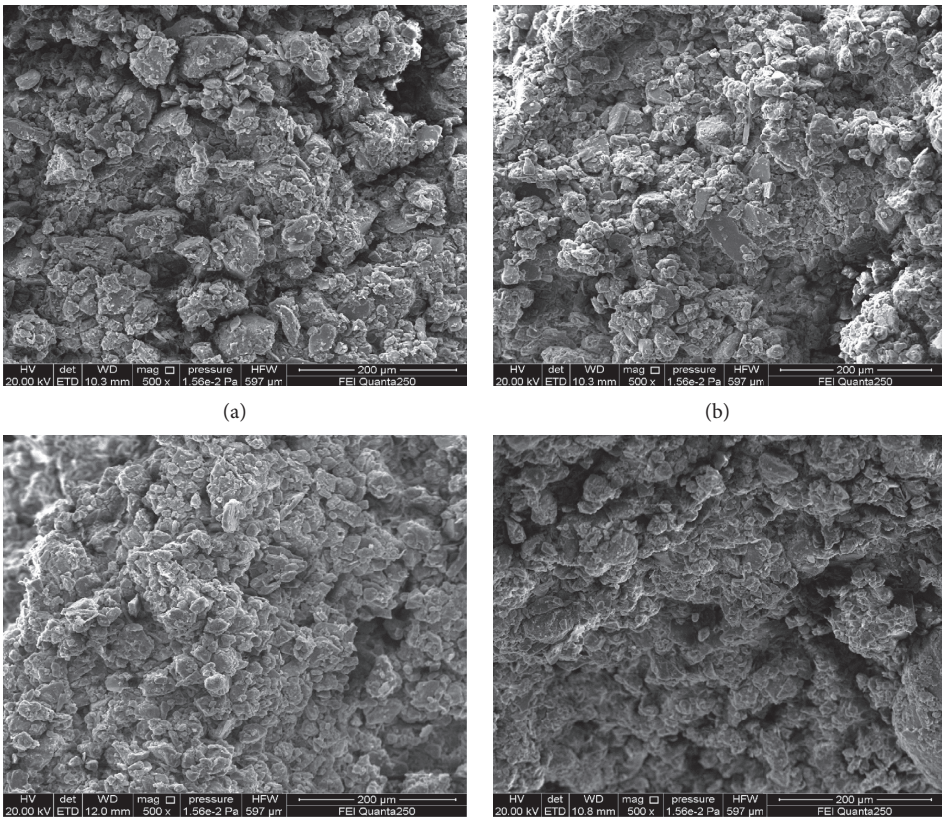

(a) (b)

(c) (d)

Figure 10: SEM image of Zhouqiao earthen soil: (a) SEM image 1, (b) SEM image 2, (c) SEM image 3, and (d) SEM image 4.

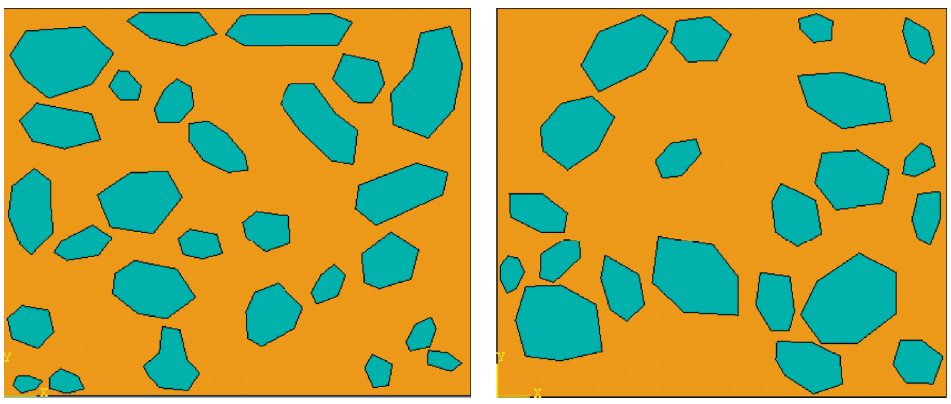

(a) (b)

Figure 11: Continued.

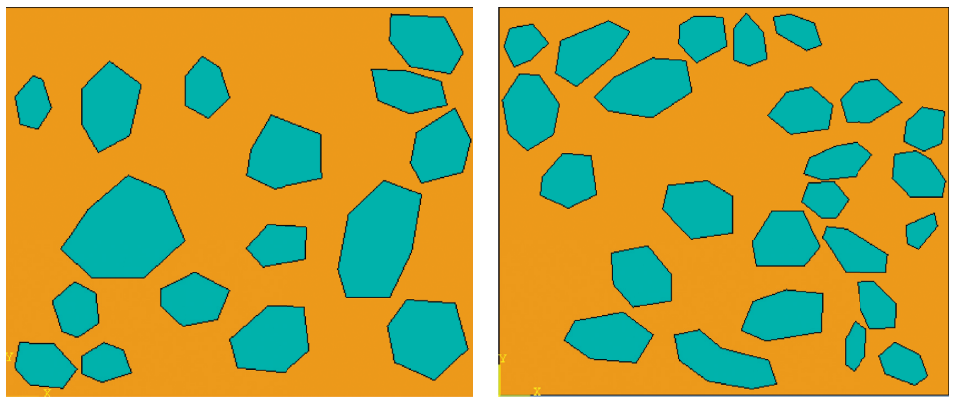

(c) (d)

Figure 11: Simulation model of the uniaxial compression test with polygonal pores: (a) simulation model 1, (b) simulation model 2, (c) simulation model 3, and (d) simulation model 4.

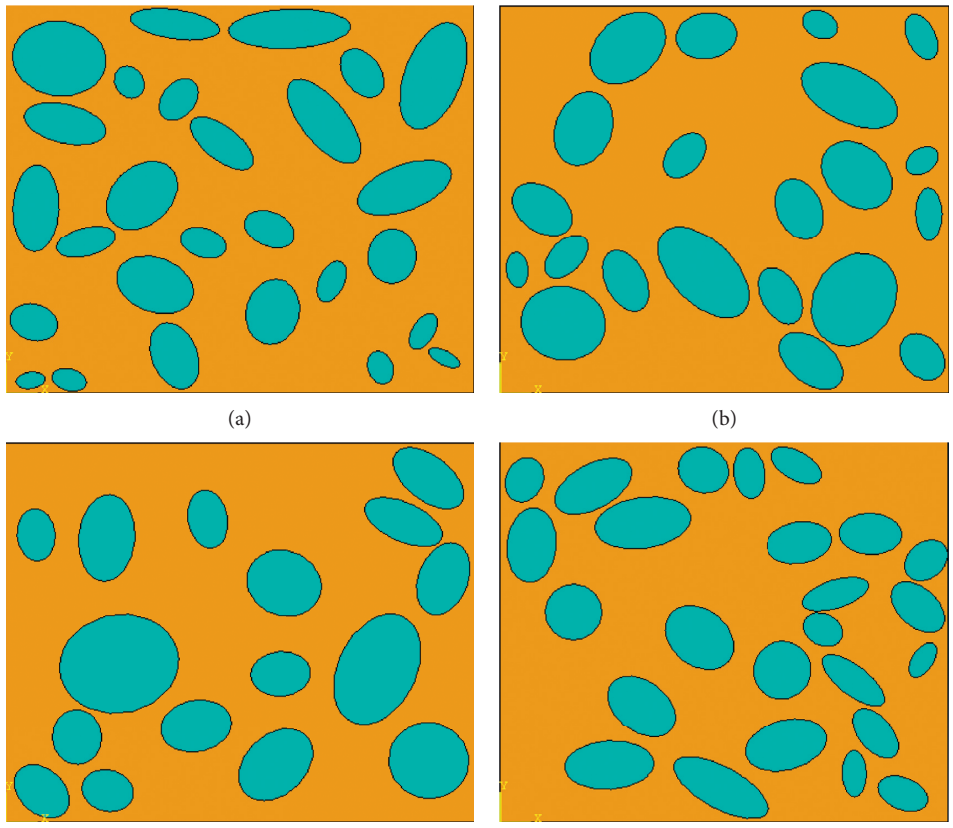

(a) (b)

(c) (d)

Figure 12: Simulation model of the uniaxial compression test with circular pores: (a) simulation model 5, (b) simulation model 6, (c) simulation model 7, and (d) simulation model 8.

change suddenly. The pore boundary of the circular pore model is smooth, the constraints between soil samples are less, and the displacement change is relatively continuous. Compared with the rubbing between soil samples and irregular particles in the polygonal pore model, the displacement change is affected by the irregular boundary, and the change is uneven. The vertical compression displacement of the circular pore model reaches 11.44e−03 mm, The displacement of polygonal pore model under vertical compression is 14.606e−02 mm, which is 1.28 times more than that of circular pore model. Through the analysis of Figures 14(b) and 15(b), it is found that the displacement of the left and right boundaries of the polygonal pore model is 3.392e−02 mm, while the displacement of the left and right

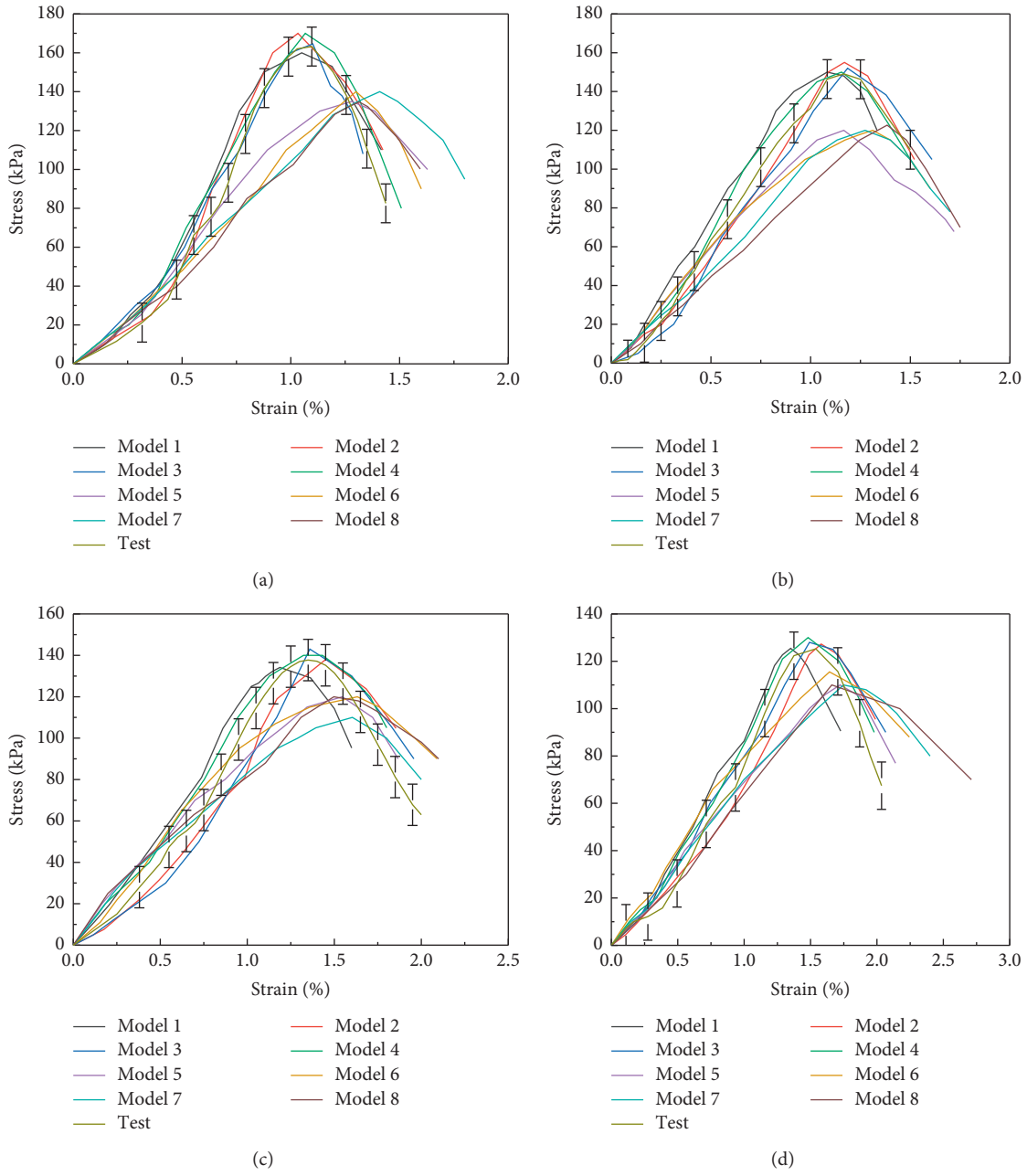

Figure 13: Stress-strain curves of macroscopic test and simulation: (a) moisture content 10%, (b) moisture content 12%, (c) moisture content 14%, and (d) moisture content 16%.

boundaries of the circular pore model is 4.266e−02 mm, which is 1.26 times more than that of the left and right boundaries of the polygonal pore model. With the increase of compressive load, the polygonal pore model is prone to stress concentration around the pores due to the irregular pore boundary. The maximum stress of the model is 3.027e−02 kPa, while the maximum stress of the circular pore model is 1.867e−02 kPa. Finally, the macroscopic response in Figure 13 is that the stress-strain curves of the circular pore model are smaller than those of the polygonal pore model.

Based on the results of the analysis of Figures 14(d) and 15(d), it can be concluded that the damage of the specimen begins to initiate and started at both ends of the bottom of the specimen. At this time, the internal cohesion of the soil facilitated the recovery from the deformation of the specimen recover, and there is, with no cracks on its surface of the specimen. With the increase of the compression load, a small number of microcracks appeared in the soil matrix, resulting in irrecoverable deformation. With the further expansion and aggregation of damage microcracks, the microcracks do not develop in a single way, but propagate microcrack

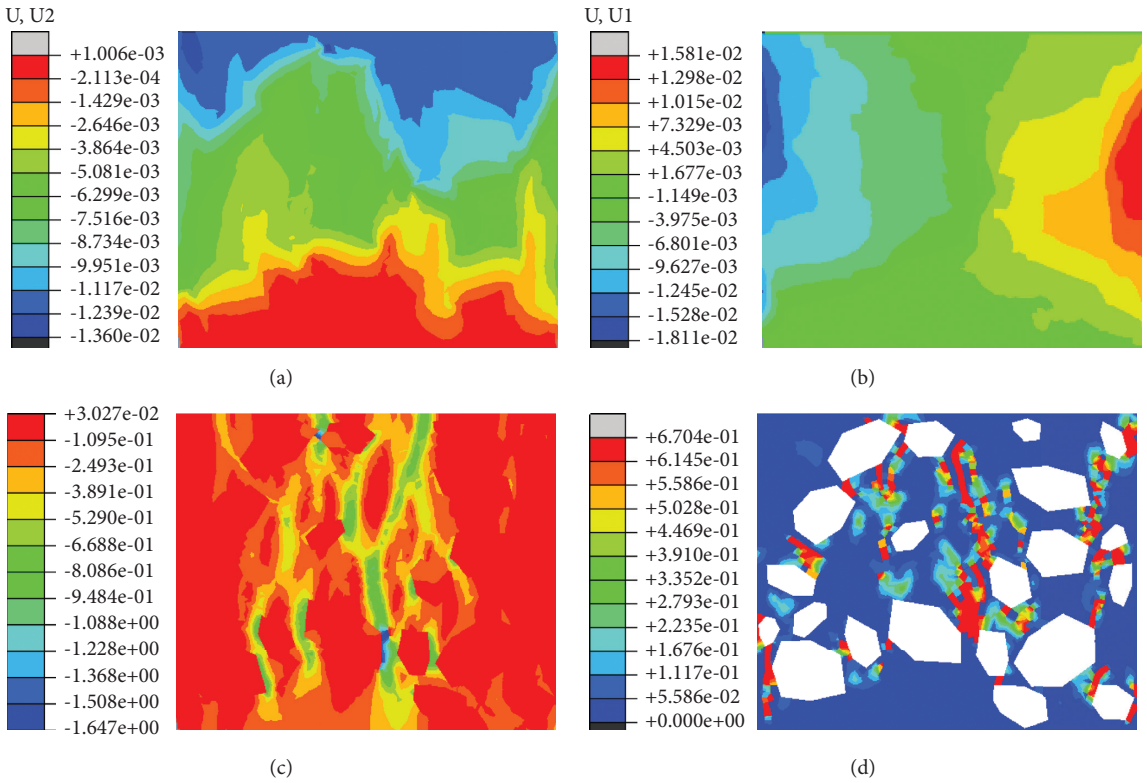

Figure 14: Model 1 simulation results: (a) displacement diagram in U2 direction, (b) displacement diagram in U1 direction, (c) axial stress diagram, and (d) damage diagram.

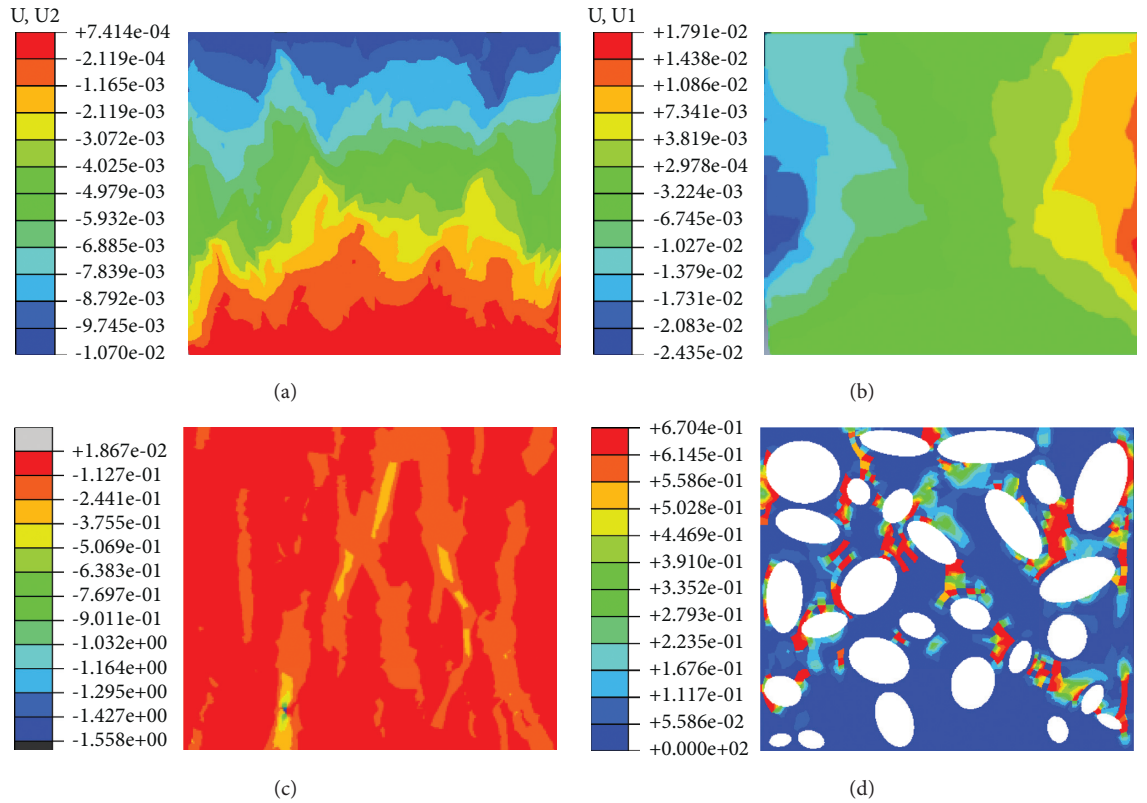

Figure 15: Model 5 simulation results: (a) displacement diagram in U2 direction, (b) displacement diagram in U1 direction, (c) axial stress diagram, and (d) damage diagram.

damages, they were simultaneously propagated along the whole section of the soil particle edge at the same time. Moreover, the damaged part of the circular pore model mostly appears between the pores, while the damaged part of the polygonal pore model not only exists between the pores but also extends to the interior of the soil sample.

5. Conclusion

The nanostructure model of site soil composed of many atoms was established by molecular dynamics method. The stress-strain relationship of different moisture content was obtained by uniaxial compression simulation. Based on the 500-fold magnified electron micrograph image and the image reconstruction method, we constructed a micromodel composed of particles, cements, and pores. The stress-strain relationship of different moisture contents of earthen soil was obtained by the displacement loading method, and the results were compared with those of the macro test. The mechanical microproperties of the cemented particles were analyzed. The aim of this study was to establish an effective method for the assessment of the safety and surface deterioration of earthen sites, which would provide a basis for follow-up research on the deterioration of earthen sites. Considering the obtained results, we can conclude that our work has met the needs and purposes of the scientific project, and a foundation has been laid for next step analysis of the deterioration effect of the environment on earthen sites and their safety evaluation. The following main conclusions have been drawn:

(1) Based on molecular dynamics simulation method, a nano structure model of Zhouqiao earthen soil composed of Si, O, Al, H, and Li atoms is established, in which water and soil are distributed in layers. By analyzing the mechanical properties of Zhouqiao earthen soil, the stress-strain relationship of site granular materials with different moisture content at nanoscale is obtained.

(2) According to the cementation characteristics of the earthen soil, it was divided into a three-phase structure composed of soil particles and pores. The shape, size, and distribution of particles were determined by SEM image reconstruction, and a micro-finite-element model reflecting real soil properties was established.

(3) Through uniaxial compression tests of the micro-finite-element model, we found that the displacement of the left and right boundaries of the circular pore model is 1.26 times more than that of the polygonal pore model, and the displacement of the polygonal pore model in vertical compression is 1.28 times more than that of the circular pore model. The simulated curve of the polygonal pore model is consistent with the test stress-strain curve, which can better reflect the change of the microstructure of the soil sample under load. There is a deviation between the results of the circular pore model and the indoor test results, but comparing the simulation results of different water content, it is found that the coincidence degree of the result curve is further increasing with the increase of the water content of the soil sample.

(4) By comparison, we found that the results of the numerical analysis were in good agreement with the results of the macrotest stress-strain curves, which indicates that the research ideas and methods in this work are feasible. We have also established a new method for difficult indoor sampling.

Data Availability

All data generated or analyzed in this study are included in this article.

Conflicts of Interest

The authors declare no conflicts of interest.

Acknowledgments

This work was supported by the National Natural Science Foundation of China (grant no. 51978634), Henan University's First-Class Discipline Cultivation Project (Science and Technology) (grant no. 2019 YLZDCG05), and Henan Province Science and Technology Development Plan Project (grant no. 212300410012).

References

[1] J. Yue, X. Huang, L. Zhao, and Z. Wang, "Study on the factors affecting cracking of earthen soil under dry shrinkage and freeze-thaw conditions," *Scientific Reports*, vol. 12, no. 1, p. 1816, 2022.

[2] Z. Zhao and Z. Sun, "Ring shear mechanical properties and numerical simulation of sand," *Chinese Journal of Underground Space and Engineering*, vol. 13, no. S1, pp. 70–74, 2017.

[3] L. Liu, L. Zhao, Y. Chen, and J. Gao, "Research progress of molecular simulation of diffusion in zeolites," *Chemical Industry and Engineering Progress*, vol. 30, no. 7, pp. 1406–1415, 2011.

[4] D. Song, J. W. Yue, J. B. Yuan et al., "Study of soil mechanical characteristics of ruins in northwest Henan Province," *Journal of Experimental Mechanics*, vol. 34, no. 1, pp. 121–130, 2019.

[5] J. W. Yue, G. H. Yang, S. Y. Wang, Y. F. Wang, and Y. F. Zhang, "Cusp catastrophe model for slope failure based on elastic slip mass," *Journal of Henan University*, vol. 49, no. 3, pp. 354–361, 2019.

[6] C.-S. Tang, Y.-J. Cui, B. Shi, A.-M. Tang, and N. An, "Effect of wetting-drying cycles on soil desiccation cracking behaviour," *Web of Conferences*, vol. 9, Article ID 12003, 2016.

[7] C. Wang, Z. Y Zhang, Y. Liu, and S. M Fan, "Geometric and fractal analysis of dynamic cracking patterns subjected to wetting-drying cycles," *Soil and Tillage Research*, vol. 170, pp. 1–13, 2017.

[8] J. Yue, X. Huang, L. Zhao, Q. Kong, Y. Chen, and Z. Wang, "Finite element method study on stress-strain relationship of site soil," *Mechanics in Engineering*, vol. 43, no. 6, pp. 921–932, 2021.

[9] M. Huang, Y. Yao, Z. Yin, and E. Liu, "An overview on elementary mechanical behaviors, constitutive modeling and

failure criterion of soils," *China Civil Engineering Journal*, vol. 49, no. 7, pp. 9–35, 2016.

[10] Z. J. Shen, "Elastic-plastic damage model of structural clay," *Chinese Journal of Geotechnical Engineering*, vol. 33, no. 4, pp. 637–642, 1993.

[11] Z. J. Shen, "Nonlinear damage mechanical model of structural clay," *Hydro-Science and Engineering*, vol. 57, no. 3, pp. 247–255, 1993.

[12] L. F. Kuang, G. Q. Zhou, X. Y. Shang, and X. D. ZHAO, "Molecular dynamic simulation of interlayer water structure in sodium montmorillonite," *Journal of China Coal Society*, vol. 38, no. 3, pp. 418–423, 2013.

[13] W. Yang, R. Chen, and X. Kang, "Application of molecular dynamics simulation method in micro-properties of clay minerals," *Chinese Journal of Geotechnical Engineering*, vol. 41, no. S1, pp. 181–184, 2019.

[14] Y. Liu, X. Yang, L. Luo, Z. Li, S. Liang, and H. Fang, "Experimental research on relationship between triaxial shear properties and microstructure of saturated soft soil," *China Journal of Highway and Transport*, vol. 32, no. 7, pp. 15–22, 2019.

[15] L. Tang, S. Cong, X. Ling, W. Xing, and Z. Nie, "A unified formulation of stress-strain relations considering micro-damage for expansive soils exposed to freeze-thaw cycles," *Cold Regions Science and Technology*, vol. 153, pp. 164–171, 2018.

[16] Y. M. Chen, P. C. Ma, and Y. Tang, "Constitutive models and hypergravity physical simulation of soils," *Chinese Journal of Theoretical and Applied Mechanics*, vol. 52, no. 4, pp. 901–915, 2020.

[17] H. Zhao, S. Jiang, Y. Ge, and C. Liu, "Molecular dynamics simulation of water molecules adsorption by different cations based montmorillonite," *SCIENTIA SINICA Technologica*, vol. 49, no. 6, pp. 703–715, 2019.

[18] T. Hu, D. Liu, and J. Chang, "Experimental study on strain rate effect of strength characteristics of unsaturated silty clay," *Case Studies in Construction Materials*, vol. 12, Article ID e00332, 2020.

[19] S. Zike, B. F. Sørensen, and L. P. Mikkelsen, "Experimental determination of the micro-scale strength and stress-strain relation of an epoxy resin," *Materials & Design*, vol. 98, pp. 47–60, 2016.

[20] J. Zhang, J.-H. Chen, and C. Edwards, "Lab NMR study on adsorption/condensation of hydrocarbon in smectite clay," *The Day*, vol. 4, no. 4, pp. 315–339, 2012.

[21] J. Li, Z. Chen, X. Li et al., "A quantitative research of water distribution characteristics inside shale and clay nanopores," *SCIENTIA SINICA Technologica*, vol. 48, no. 11, pp. 1219–1233, 2018.

[22] D. L. Bish, "Rietveld refinement of non-hydrogen atomic positions in kaolinite," *Clays and Clay Minerals*, vol. 37, no. 4, pp. 289–296, 1989.

[23] D. Hou, Y. U. Jiao, J. Zhang et al., "Insights on hydrolysis weakening of calcium silicate hydrate: a ReaxFF molecular dynamics study," *Journal of Hydraulic Engineering*, vol. 52, no. 1, pp. 34–41, 2021.

[24] H. F. Xu, H. J. Wu, S. P. Guo, and T. P. Liao, "Study on the parameters of pile soil contact surface element," *Exploration Engineering(rock and Soil Drilling and Tunneling)*, vol. 29, no. 5, pp. 10–12, 2002.

[25] Y. Zhang, C. Y. Liu, Y. Y. Wang, and H. Yin, "Mesoscale modeling based numerical study on size effect of concrete compressive strength," *Journal of Building Structures*, vol. 38, no. S1, pp. 493–501, 2017.

[26] H. P. Feng, D. L. Ma, Q. Y. Liu, and C. L. YE, "Method for calculating three dimensional apparent porosity of soils based on SEM images," *Chinese Journal of Geotechnical Engineering*, vol. 41, no. 3, pp. 574–580, 2019.

[27] M. J. Jiang, C. H. Li, W. Liu, A. Zhang, and X. W. Zhang, "Extension and compression tests mechanical behaviors of bonded granules with different bond widths," *Chinese Journal of Geotechnical Engineering*, vol. 40, no. S2, pp. 12–16, 2018.

[28] M. Li and H. N. Li, "Investigation into dynamic properties of damaged plasticity model for concrete in ABAQUS," *Journal of Disaster Prevention and Mitigation Engineering*, vol. 31, no. 3, pp. 299–303, 2011.